ACS Macro Letters

pubs.acs.org/macroletters Letter

Tailoring the Interplay between Two Monomers in the Properties of Degradable Polyesters Synthesized via Ring-Opening Alternating Copolymerization

Sumin Lee, Woo Hyuk Jung, Minseong Kim, Dong June Ahn, and Byeong-Su Kim*

Cite This: ACS Macro Lett. 2023, 12, 590−597 Read Online

ACCESS | Metrics & More | Article Recommendations | Supporting Information

ABSTRACT: Ring-opening alternating copolymerization (ROAC) of cyclic anhydrides and epoxides has emerged as a powerful strategy to produce degradable polyesters with a diverse array of structures from the combination of two distinct building blocks. In this work, we exploited the organocatalytic ROAC of cyclic anhydrides and a functional epoxide, *t*-butyl glycidoxy acetate, followed by acidic deprotection to access degradable polyesters with carboxylic acid pendants. To study the interplay between monomers, diglycolic anhydride and glutaric anhydride were used as cyclic anhydrides to prepare two polyesters. In particular, the effects of the oxygen heteroatom in the cyclic anhydrides on the properties of the carboxylic acid-containing polyesters were investigated. The introduction of the oxygen heteroatom into the cyclic anhydrides significantly influenced their thermal properties and pH-dependent self-association behavior in an aqueous solution. Furthermore, molecular dynamics simulations elucidate that the number and type of hydrogen bonds play a crucial role in the self-association behavior between the polymers both in the solution and bulk states. The findings of this study highlight the importance of the interplay between monomers in the design of functional polyesters with tunable properties.

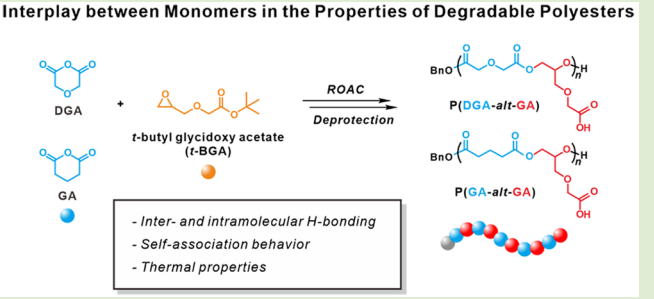

The continuously increasing environmental pollution caused by nondegradable petroleum-based plastics has become a global issue.[1] Recently, degradable polymers have emerged as suitable alternatives to nondegradable plastics owing to their advantageous properties, especially their ability to degrade at a faster rate without causing significant environmental concerns. Aliphatic polyesters are sustainable alternatives because of their numerous renewable sources, facile hydrolytic degradation, and high biocompatibility.[2] Consequently, they are widely used in packaging, tissue engineering, and biomedical devices.[3−5]

Among the well-known synthetic routes to polyesters, the step-growth approach has reached maturity; however, it typically requires harsh conditions and the removal of byproducts. Ring-opening polymerization (ROP) of lactones has also been studied extensively, although the resulting polyesters have a limited range of properties, owing to the minimal functional diversity of the available lactones. An alternative chain-growth route to polyesters is the ring-opening alternating copolymerization (ROAC) of cyclic anhydrides and epoxides.[6−8] The combinations of two distinct monomers enable the production of degradable polyesters with a diverse array of structures.

One appealing aspect of the ROAC of cyclic anhydrides and epoxides is the use of two types of monomers, which facilitate the synthesis of polymers with wide structural diversity. To date, several commercially available monomers, such as propylene oxide, cyclohexene oxide, and phthalic anhydride, have been widely studied. Interestingly, further advancements have made it possible to explore more functionally diverse monomers for achieving polyesters with specific functionalities. As a representative example, Coates and co-workers synthesized renewable tricyclic anhydrides and copolymerized them with propylene oxide and cyclohexene oxide to tune the glass-transition temperature (T_g) of the polymers and enhance their sustainability.[9] Moreover, the ROAC of a D-xylose-based oxetane with cyclic anhydrides was demonstrated to synthesize an array of sugar-based polyesters, which were amenable to further postpolymerization functionalization through the hydroxyl group and internal alkene.[10] The recent study of copolymerization of fatty acid-based epoxides and various cyclic anhydrides afforded functional polyesters, which can form rigid macromolecular networks upon subsequent cross-linking processes.[11] However, systematic studies used to investigate the influence of the interplay between two

Received: February 19, 2023
Accepted: April 11, 2023

https://doi.org/10.1021/acsmacrolett.3c00104
ACS Macro Lett. 2023, 12, 590−597

Scheme 1. Ring-Opening Alternating Copolymerization (ROAC) of Cyclic Anhydrides and *t*-BGA Catalyzed by a *t*-BuP$_1$/TEB Pair[a]

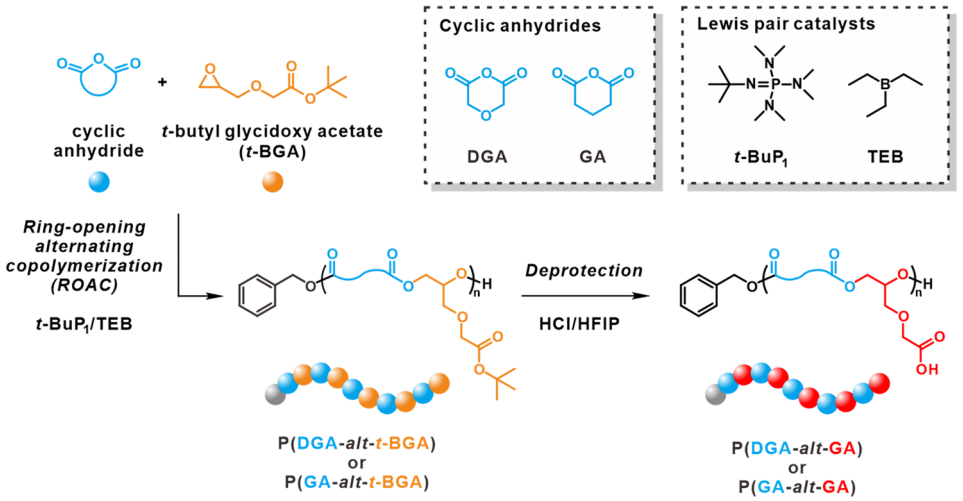

[a]See the Supporting Information for details of the polymer structures.

monomers on the chemical and physical properties of polyesters are scarce.

In this context, it is essential to develop functional monomers to tailor the characteristics of polyesters using ROAC. As a part of our ongoing effort in the development of functional epoxide monomers,[12−16] *t*-butyl glycidoxy acetate (*t*-BGA) was designed to produce a carboxylic acid-functionalized polyether.[17] Polymers bearing carboxylic acid groups are useful because of their versatile applications in pH-responsive drug delivery systems,[18] hydrogels,[19] self-healing materials,[20] adhesives,[21] and battery binders.[22] Thus, we envision that the synergistic interplay between the monomers influences the properties of polyesters synthesized via the ROAC of various anhydrides with functional epoxide monomers.

Herein, we present the synthesis of degradable polyesters with carboxylic acid pendants via the ROAC of cyclic anhydrides and *t*-BGA using benzyl alcohol as an initiator and a mild phosphazene base (*t*-BuP$_1$) and triethylborane (TEB) as Lewis pair catalysts (Scheme 1). Diglycolic anhydride (DGA) and glutaric anhydride (GA) were used as cyclic anhydrides, which afforded two different polyesters, P(DGA-*alt*-*t*-BGA) and P(GA-*alt*-*t*-BGA), respectively. After the cleavage of the *t*-butyl ester protecting groups, we obtained the desired carboxylic acid-containing polyesters, P(DGA-*alt*-GA) and P(GA-*alt*-GA).

The impact of oxygen heteroatoms present in cyclic anhydrides on the properties of the resulting polyesters was investigated. The introduction of oxygen heteroatoms significantly influenced the thermal properties and pH-dependent self-association in an aqueous solution. Notably, the number and lifetime of hydrogen bonds (H-bonds) according to the types of interactions between the functional moieties were further analyzed via molecular dynamics (MD) simulations of the solution and bulk states. Finally, the degradability of the polyesters was evaluated under basic conditions.

To prepare carboxylic acid-containing polyesters via ROAC of cyclic anhydrides and *t*-BGA, we initially optimized the reaction conditions using a Lewis pair catalyst consisting of *t*-BuP$_1$ and TEB. Specifically, the effects of the catalyst ratio, reaction medium, temperature, and reaction time on the polymerization were investigated. As a model reaction, the ROAC of DGA and *t*-BGA was performed using benzyl alcohol (BA) as an initiator. The molar feed ratio of BA and monomers (i.e., $[BA]_0/[DGA]_0/[t\text{-}BGA]_0$) was fixed at 1/50/100. Our first attempt using 1 equiv of *t*-BuP$_1$ (relative to the hydroxyl group of BA) without TEB in the bulk at 25 °C (entry 1 in Table S1 in the Supporting Information) was unsuccessful, suggesting that the basicity of *t*-BuP$_1$ cannot induce a self-buffering mechanism that renders the carboxy and hydroxy terminals active to allow chain growth.[23−25]

We thus performed polymerization with varying ratios of $[t\text{-}BuP_1]_0/[TEB]_0$ in the bulk at 25 °C (entries 2−4 in Table S1) while monitoring the conversion of the monomer, molecular weight, and dispersity of the resulting polymers by withdrawing aliquots at predetermined time intervals. Using 1 equiv of *t*-BuP$_1$ and 2 equiv of TEB with regard to BA, the conversion of DGA reaches 65 and >99% in 8 and 20 h, respectively (entry 2 in Table S1). This result suggests that the ROAC of DGA and *t*-BGA is affordable at 25 °C by the cooperative catalysis of *t*-BuP$_1$ and TEB, likely through the activation of chain ends (carboxyl and hydroxyl) by *t*-BuP$_1$ and the activation of *t*-BGA by TEB. However, when the amount of TEB is increased to 4 equiv of BA at a fixed *t*-BuP$_1$, the reaction proceeds much slower as more than 20 h is needed to reach complete DGA conversion (entry 3 in Table S1). This is probably because catalyst binding to the cyclic anhydride causes a decrease in the polymerization rate via competitive inhibition. Entry 4 in Table S1 performed with an $[t\text{-}BuP_1]/[TEB]$ ratio of 0.5/2 shows that the copolymerization rate is noticeably low due to the decreased chain-end nucleophilicity. Furthermore, the reaction rate became slower in THF and the conversion of DGA was lower than that in the bulk, while other conditions are fixed (entry 5 in Table S1).

Furthermore, as the reaction time was increased, the dispersity increased, indicating that transesterification occurred; for example, as the reaction time was increased from 8 to 20 h, the molecular weight dispersity ($Đ$) increased from 1.15 to 1.23 (entry 2 in Table S1). When the reaction continued beyond >99% monomer conversion, it was found that $M_{n,GPC}$ tended to decrease under some conditions. According to the literature, the chain scission of polyester

https://doi.org/10.1021/acsmacrolett.3c00104
ACS Macro Lett. 2023, 12, 590−597

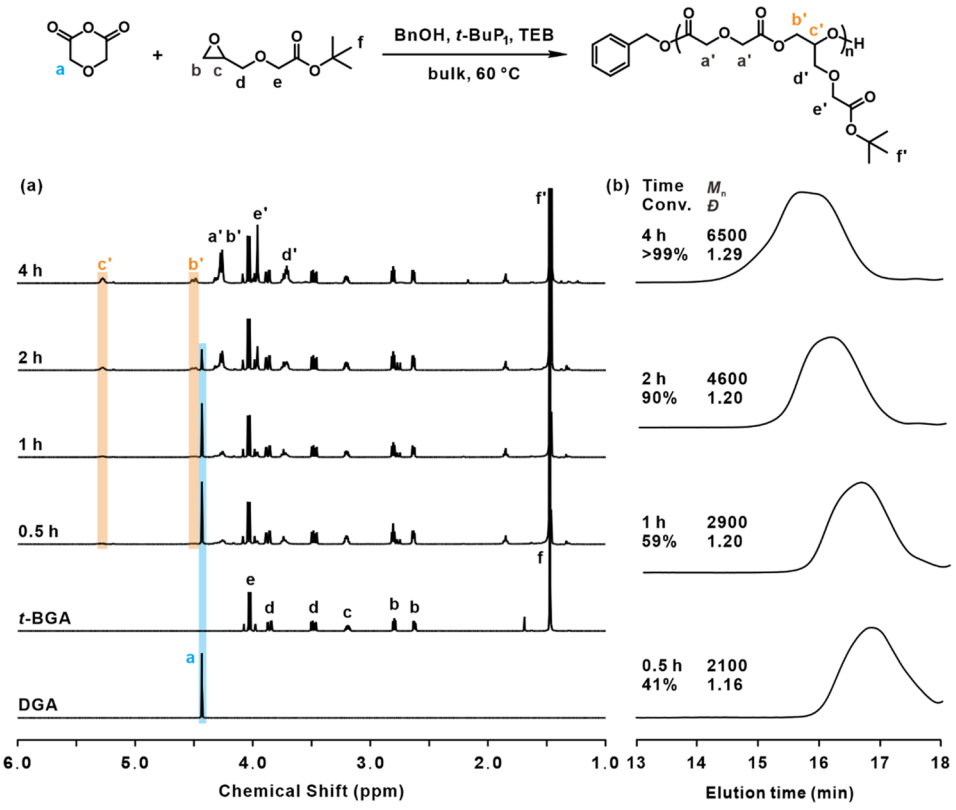

Figure 1. (a) Stacked ^{1}H NMR spectra and (b) evolution of the GPC traces of the crude reaction mixture collected from the copolymerization of DGA and *t*-BGA at different reaction times (Table S2 in the Supporting Information). ^{1}H NMR spectra were collected in $CDCl_3$, and GPC analyses were performed in THF with a PS standard.

was observed via a base-catalyzed hydrolysis mechanism, which possibly suggests chain scission under a prolonged reaction time.[26]

Next, polymerization was conducted at 60 °C while keeping all of the other conditions fixed. In this case, the overall reaction rate accelerated, and the highest molecular weight of 8.0 kg mol^{-1} was obtained in 4 h (entry 8 in Table S1). Considering the reaction time, molecular weight, and dispersity, in this study, the optimal condition for ROAC was set to an initiator-to-catalyst ratio of $[BA]_0/[t\text{-}BuP_1]_0/[TEB]_0$ = 1/1/4 in the bulk at 60 °C.

The polymerization was examined at shorter time intervals under the optimized conditions. Figure 1a shows the stacked ^{1}H NMR spectra of the reaction mixture from the copolymerization of DGA and *t*-BGA (Table S2). Upon polymerization, the proton signal representing DGA at 4.43 ppm (*a* peak) decreases while signals corresponding to P(DGA-*alt*-*t*-BGA) at 5.34 and 5.27 ppm (*c*′ peak) and 4.58 and 4.49 ppm (*b*′ peak) appear. As shown in Figure 1b, the GPC traces indicate that the molecular weight of P(DGA-*alt*-*t*-BGA) shifts to a lower elution time, suggesting chain growth during polymerization.

Furthermore, the copolymerization of GA and *t*-BGA was examined under the optimized conditions via ^{1}H NMR and GPC analyses (Figure S2 and Table S2). Upon polymerization, the proton signals representing GA at 2.75 ppm (*a* peak) and 2.01 ppm (*b* peak) decrease while those representing P(GA-*alt*-*t*-BGA) at 5.28−5.15 ppm (*d*′ peak), 4.47−4.34 ppm (*c*′ peak), and 4.23−4.11 (*c*′ peak) appear. The molecular weight of P(GA-*alt*-*t*-BGA) increased as the polymerization proceeded, which supports the controlled chain growth during propagation.

Interestingly, we found that the reactivity of the DGA monomer was higher than that of GA during ROAC, considering a higher conversion under identical reaction conditions. This higher reactivity of DGA can be mainly attributed to the ring strain and nucleophilicity of anhydride carboxylate as recently demonstrated in the literature.[27,28]

According to previous studies, when the ROAC reaction is catalyzed by the *t*-BuP_1/TEB pair and the equivalence of epoxide is typically in excess compared to that of cyclic anhydride, polyether blocks begin to form after all of the cyclic anhydrides are consumed during the synthesis of the polyester.[29] Recently, it was found that the copolymerization of cyclic anhydride and excess epoxide at elevated temperatures was free of polyether formation when catalyzed by the *t*-BuP_1/TEB pair, even after complete anhydride consumption.[30] In the case of ROAC utilizing DGA and *t*-BGA, approximately 46% of the polyether segment (vs 54% of the polyester segment) was generated when the reaction was prolonged for 20 h to realize a full monomer conversion (>99%) (Figure S3). As such, we halted the ROAC for 2 and 3 h for DGA and GA, respectively, to limit the monomer conversion below 95% to minimize the generation of the polyether segment.

Meanwhile, the copolymerization was performed using equivalent amounts of the two monomers in bulk at 60 °C with a ratio of $[BA]/[t\text{-}BuP_1]/[TEB]/[DGA]/[t\text{-}BGA]$ at 1/1/4/50/50 for 22 h. The ^{1}H NMR spectrum of the isolated product did not indicate the formation of the polyether segment (Figure S4a). However, it was found that the feed

https://doi.org/10.1021/acsmacrolett.3c00104
ACS Macro Lett. 2023, 12, 590−597

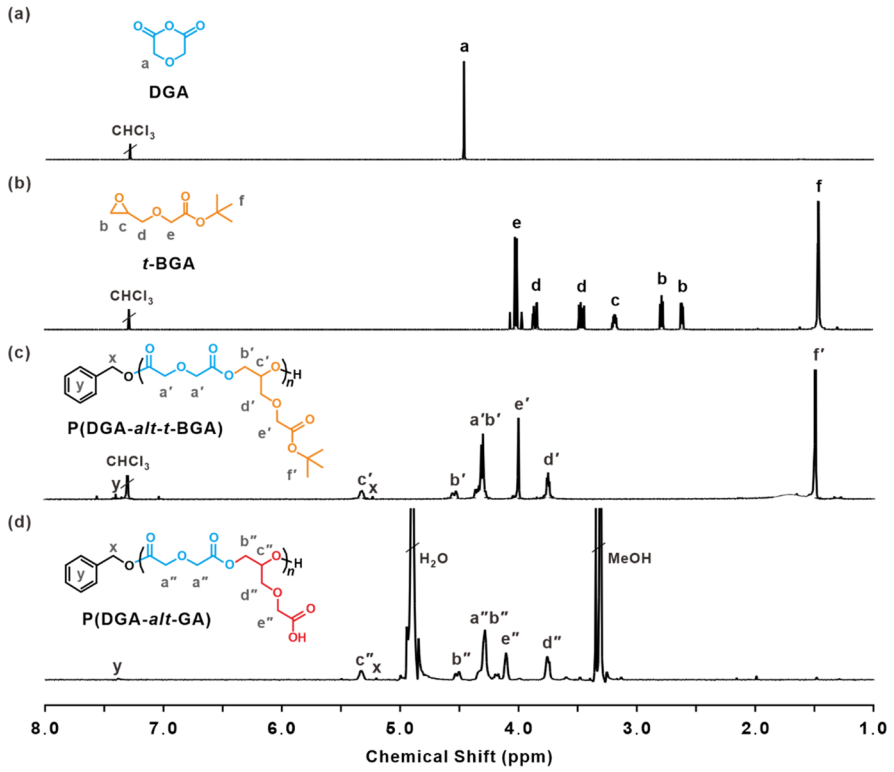

Figure 2. Representative ^{1}H NMR spectra of the (a) DGA monomer, (b) *t*-BGA monomer, (c) P(DGA-*alt*-*t*-BGA), and (d) deprotected P(DGA-*alt*-GA). All spectra were collected in $CDCl_3$ except for panel (d) acquired in CD_3OD.

Table 1. Characterization of the Synthesized Polyesters[a]

Polyester	Time (h)	Conv. (%)[b]	$M_{n,theo}$ (kg mol^{-1})[c]	$M_{n,GPC}$ (kg mol^{-1})[d]	$M_{n,GPC}$ (kg mol^{-1})[e]	$Đ^d$	$Đ^e$	T_g (°C)	T_g (°C)[f]
P(DGA-*alt*-*t*-BGA)	2	92	14.1	5.2	14.4	1.22	1.24	15.4	35.1
P(GA-*alt*-*t*-BGA)	3	66	10.1	4.2	11.0	1.16	1.25	−7.2	−3.7

[a]Polymerization conditions: $[OH]_0/[t\text{-BuP}_1]_0/[TEB]_0/[DGA]_0/[t\text{-BGA}]_0$ = 1/1/4/50/100, bulk, 60 °C. [b]Conversion of cyclic anhydride calculated from ^{1}H NMR spectra of the crude product. [c]Calculated using $[anhydride]_0/[I]_0 \times$ Conv. × (M.W. of anhydride + M.W. of epoxide) + (M.W. of initiator). [d]Obtained from GPC analysis (THF, PS standards) of the isolated product. [e]Obtained from GPC analysis (DMF, PS standards) of the isolated product. [f]The deprotected polyester. See the Supporting Information for the full list of polymers synthesized.

ratio of the two monomers influences the relative polymerization rate (Figure S4b).

As shown in Figure 2, the ^{1}H NMR spectra indicate that the conversion of the monomer to the polymer is accompanied by the disappearance of the epoxide peaks at 2.62, 2.81 (*b* peaks), and 3.20 ppm (*c* peak) upon polymerization. The peaks of isolated P(DGA-*alt*-*t*-BGA) could be clearly assigned along with the methylene protons in the benzyl ester at 5.1 ppm (*x* peak) in Figure 2c. Likewise, the peaks of isolated P(GA-*alt*-*t*-BGA) were assigned with the methylene protons in benzyl ester (Figure S5).

The obtained number-average molecular weight (M_n) of the polyesters varies from 4.2 to 5.2 kg mol^{-1}, with the molecular weight dispersities ($Đ$) of 1.16 and 1.22 based on the GPC measurements in THF. The results obtained from the GPC measurements in DMF were almost consistent with the theoretical values, indicating 14.4 and 11.0 kg mol^{-1}, with molecular weight dispersities ($Đ$) of 1.24 and 1.25, respectively. These results prove that all of the synthesized polyesters had similar molecular weights and comparable molecular weight distributions (Table 1). To further identify whether both monomers were involved in the formation of the copolymers, we analyzed each polyester by ^{1}H DOSY-NMR. A single diffusion coefficient was obtained for each polymer, revealing the successful copolymerization of the polyester via ROAC (Figure S6).

Matrix-assisted laser desorption/ionization time-of-flight (MALDI-ToF) measurements were performed to confirm the chemical structure of the obtained polymer (Figure S7). The MALDI-ToF spectrum of P(DGA-*alt*-*t*-BGA) displays a major mass distribution with a constant interval of 304.29 g mol^{-1}, corresponding to the sum of the molecular weights of the two monomers, demonstrating the alternating structure of the polyester. Specifically, a representative mass spectrum with the observed molecular weight of 2189.28 g mol^{-1} corresponds to the BnOH-initiated polymer with the *t*-BGA end group without one *t*-butyl group with Na^+ as the counterion. Similarly, P(GA-*alt*-*t*-BGA) shows an alternating structure of the resulting polyester, demonstrating the major series with a constant spacing of 302.32 g mol^{-1}, corresponding to the sum of the molecular weights of the two monomers. Moreover, a representative mass spectrum with the observed molecular weight of 2946.58 g mol^{-1} matches the BnOH-initiated polymer with a GA end group.

Subsequently, the deprotection was followed by treatment with HCl in hexafluoroisopropyl alcohol (HFIP) to produce the desired polyesters with carboxylic acid pendants. Compared to the common trifluoroacetic acid treatment, the

https://doi.org/10.1021/acsmacrolett.3c00104
ACS Macro Lett. 2023, 12, 590−597

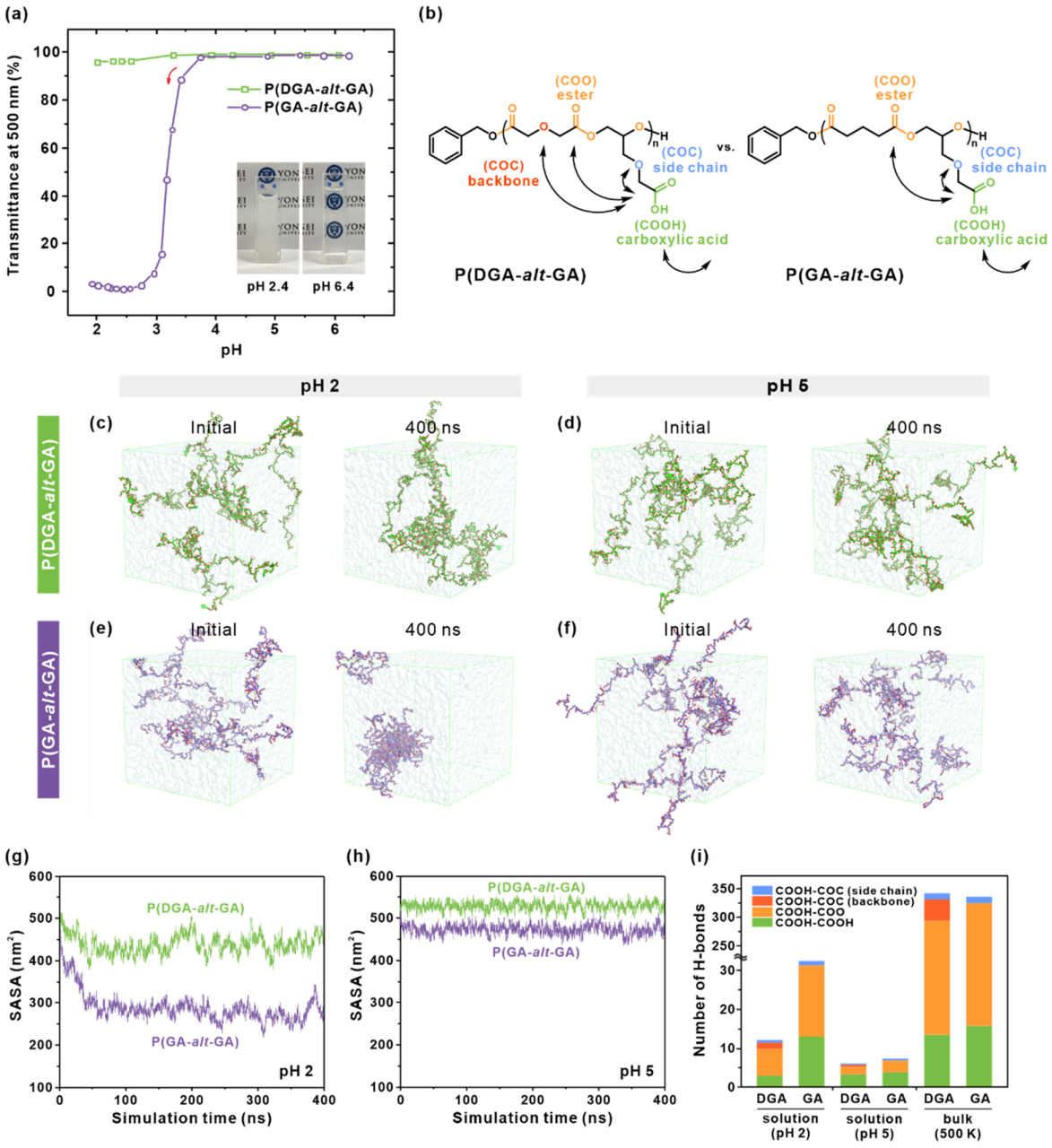

Figure 3. (a) Changes in the transmittance of the aqueous P(DGA-*alt*-GA) and P(GA-*alt*-GA) solutions at 500 nm under varying pH conditions. The concentration of the polymers was set at 5 mg mL^{-1}. The inset image corresponds to the P(GA-*alt*-GA) solution at pH 2.4 and 6.4. (b) Various types of interactions between the functional groups of P(DGA-*alt*-GA) and P(GA-*alt*-GA). (c–f) All-atom molecular dynamics (MD) simulations of the aqueous solution of P(DGA-*alt*-GA) and P(GA-*alt*-GA) at pH 2 and 5. (Left) Initial and (right) final configurations of the P(DGA-*alt*-GA) solution at (c) pH 2 and (d) pH 5. (Left) Initial and (right) final configurations of the P(GA-*alt*-GA) solution at (e) pH 2 and (f) pH 5. (g, h) Time-lapsed solvent-accessible surface area (SASA) of the P(DGA-*alt*-GA) and P(GA-*alt*-GA) solutions at (g) pH 2 and (h) pH 5. (i) Number of H-bonds according to the types of interactions between the functional groups of P(DGA-*alt*-GA) and P(GA-*alt*-GA) under different conditions. Refer to the notation presented in panel (b) for different H-bonding types.

combination of HCl with HFIP exhibited a fast and complete removal of the *t*-butyl groups.[31] We thus exploited the HCl/HFIP deprotection process to cleave the *t*-butyl groups in both P(DGA-*alt*-*t*-BGA) and P(GA-*alt*-*t*-BGA) to yield P(DGA-*alt*-GA) and P(GA-*alt*-GA), respectively. In our case, the reaction was completed within 1 h, which is indicated by the disappearance of the characteristic *t*-butyl proton signal at 1.46 ppm (Figure 2d and Figure S5). Notably, no noticeable degradation of the polyester backbone was observed, as confirmed by the ^{1}H DOSY-NMR spectra of P(DGA-*alt*-GA) and P(GA-*alt*-GA), which showed a single diffusion coefficient (Figure S6). In addition, both polymers were viscous oils before the deprotection; however, an apparent difference was observed between the two samples upon deprotection. For instance, P(DGA-*alt*-GA) showed a glassy phase, whereas P(GA-*alt*-GA) displayed a rubbery phase at room temperature.

In all cases, changes in the characteristic functional moieties were clearly observed via FT-IR analysis. For example, the disappearance of the *t*-butyl peak at 1368 cm^{-1} revealed that

https://doi.org/10.1021/acsmacrolett.3c00104
ACS Macro Lett. 2023, 12, 590−597

polymerization upon deprotection results in the desired polyesters with carboxylic acid groups (Figure S8).

The T_g of the polyesters both before and after deprotection was analyzed by differential scanning calorimetry (DSC). No melting or crystallization peaks were identified for these polymers, suggesting their amorphous nature. Before deprotection, P(DGA-*alt*-*t*-BGA) exhibited a higher T_g of 15.4 °C compared to −7.2 °C for P(GA-*alt*-*t*-BGA) (Table 1). This observed T_g difference can be attributed to the presence of a more electronegative oxygen atom within the structure of the cyclic anhydride, which facilitates stronger intermolecular interactions in P(DGA-*alt*-*t*-BGA). After the deprotection of the *t*-butyl groups, the T_g of the carboxylic acid-containing polyesters significantly increased to 35.1 °C for P(DGA-*alt*-GA) and −3.7 °C for P(GA-*alt*-GA) due to the introduction of the carboxylic acid functional groups for H-bonding in the polymer chains. It is also of note that the difference in the T_g value change upon deprotection of P(DGA-*alt*-GA) (ΔT_g = 19.7 °C) was higher than that of P(GA-*alt*-GA) (ΔT_g = 3.5 °C). This behavior can be attributed to the cooperative H-bonding interactions in P(DGA-*alt*-GA), including those between the carboxylic acid in the side chain (H-bonding donor) and the oxygen heteroatoms in the polyester backbone (H-bonding acceptor).

Subsequently, the self-association of aqueous solutions of P(DGA-*alt*-GA) and P(GA-*alt*-GA) was investigated under varying pH conditions. The transmittance of the polymer solution was measured via UV/vis spectroscopy while increasing the degree of protonation by the gradual addition of dilute HCl solution. Interestingly, the transmittance of the P(GA-*alt*-GA) solution remained steady before sharply dropping to 0% at pH 2.5, whereas the P(DGA-*alt*-GA) solution demonstrated a negligible change in transmittance upon pH changes (Figure 3a). Similar to the self-association behavior of the polyether with carboxylic acid pendants demonstrated in our previous study,[17] the inter- and intramolecular H-bonding between the polyether backbone and the carboxylic acid pendant groups was found to be responsible for the observed self-association behavior under acidic conditions. We also checked the stability of the polyester backbone in aqueous solutions at pH 2 and 6. As shown in Figure S9, there was no significant degradation after 3 days. Moreover, the reversibility of the self-association behavior was clearly demonstrated in the aqueous P(GA-*alt*-GA) solution with cycles of alternate addition of 0.1 M NaOH or 0.1 M HCl.

To unveil the differences between the self-association behaviors of P(DGA-*alt*-GA) and P(GA-*alt*-GA) at the molecular level, we performed all-atom molecular dynamics (MD) simulations of the systems containing eight polymer chains of P(DGA-*alt*-GA) and P(GA-*alt*-GA) under different pH conditions (Figure 3c−f). In the fully protonated P(DGA-*alt*-GA) system at pH 2, some polymers remained separated until the end of the 400 ns simulation (Figure 3c). Meanwhile, all of the polymers in the fully protonated P(GA-*alt*-GA) system at pH 2 became organized into a large single cluster by the end of the simulation (Figure 3e). This result is consistent with that obtained from the experiments. We then conducted simulations of the polymer solutions at pH 5 to verify the effect of pH on the self-association process (Figure 3d, f). In this case, half of the carboxylic acid moieties were assumed to be deprotonated on the basis of the pK_a values of common carboxylic acid groups (pK_a ∼5 to 6). No cluster formation was observed in either system, following the 400 ns simulation due to the repulsion between the negative charges of the carboxylic acid groups. Furthermore, the solvent-accessible surface area (SASA) was calculated to quantitatively confirm the aggregation tendency of the polymers (Figure 3g, h). Evidently, the SASA of P(GA-*alt*-GA) was approximately half of that of P(DGA-*alt*-GA) at pH 2. These results again indicate that the self-association in P(GA-*alt*-GA) is more pronounced than that in P(DGA-*alt*-GA) in concert with the experimental results.

Furthermore, in order to determine the effect of H-bonding on the self-association behavior, we calculated the number and lifetime of H-bonds according to the types of interactions between the functional groups of P(DGA-*alt*-GA) and P(GA-*alt*-GA) under different conditions (Figure 3b, i and Table S3). The number of H-bonds in P(DGA-*alt*-GA) is expected to be higher because the polymer backbone includes carboxylic acid pendants and oxygen heteroatoms, which can exhibit cooperative H-bonding interactions. However, the number of H-bonds formed between the polymers was found to be 12.12 for P(DGA-*alt*-GA) and 32.43 for P(GA-*alt*-GA) in the solution states at pH 2, respectively. This unexpected influence was evident from the number of H-bonds formed between the polymers and the water molecules. Specifically, the number of H-bonds formed between the polymer and the water molecules was considerably higher in P(DGA-*alt*-GA) (986.6) than in P(GA-*alt*-GA) (735.4). As the oxygen heteroatoms in the polyester backbone induced more hydrogen bonding with the water molecules, they prohibited the formation of hydrogen-bonding networks in the P(DGA-*alt*-GA) polymer chains in the solution state. Moreover, the number of H-bonds formed between the polymers was significantly lower at pH 5 than at pH 2. Taken together, we propose that the stronger H-bonding networks formed in P(GA-*alt*-GA) originate from the carboxylic acid and ester backbone (i.e., COOH−COO) and the carboxylic acid (i.e., COOH−COOH)-induced self-association process at pH 2.

We extended the MD simulation to extract more detailed descriptors to understand the different behaviors of the two polyesters in a bulk state, including the number and lifetime of H-bonds, T_g, the diffusion coefficient, the fractional free volume, and solubility parameters (Figure 3i, Figure S10, and Table S4). In the bulk state at 500 K, P(DGA-*alt*-GA) possessed a slightly higher number of H-bonds than did P(GA-*alt*-GA) due to the additional interactions between carboxylic acid and the ether backbone (i.e., COOH−COC). Notably, the simulated T_g value is different from the T_g value obtained from the DSC analysis. However, the difference between T_g of the two polyesters P(DGA-*alt*-GA) and P(GA-*alt*-GA) is in close agreement with each other (Figure S10). The difference between the two polyesters is further highlighted by the diffusion coefficient and fractional free volume of the systems shown in Table S5. Furthermore, the solubility parameter (δ), which is defined as the square root of the cohesive energy density, can act as an indicator of the intermolecular interactions of the polymers. The solubility parameters of P(DGA-*alt*-GA) are higher than those of P(GA-*alt*-GA), demonstrating that P(DGA-*alt*-GA) exhibits stronger intermolecular interactions, owing to the presence of oxygen atoms in the DGA monomer. In concert with our results, Tian et al. recently demonstrated that heteroatoms within polyesters enhance their thermal and gas barrier properties.[32] These results validate the formation of stronger inter- and intra-

https://doi.org/10.1021/acsmacrolett.3c00104
ACS Macro Lett. 2023, 12, 590−597

molecular H-bonding networks in P(DGA-*alt*-GA) in the bulk state, in contrast to that observed in the solution state.

Finally, the prepared polyesters were subjected to basic conditions (0.25 M NaOD in D_2O) to confirm their degradability at 25 °C. It was found that the polyesters readily degraded into the corresponding monomer derivatives, as determined by ^{1}H NMR spectra (Figure S11).

In summary, we synthesized polyesters with carboxylic acid pendants via ROAC of cyclic anhydrides and *t*-BGA. To study the interplay between monomers, we used DGA and GA as cyclic anhydrides. The effects of oxygen heteroatoms on the properties of the resulting polyesters were investigated by a combination of experiments and MD simulations. The self-association behavior of P(GA-*alt*-GA) in the solution state at pH 2 was induced by the larger H-bonds that originated from the carboxylic acid and ester backbone as well as the carboxylic acid moieties. Meanwhile, stronger intermolecular interactions were observed in the bulk state of P(DGA-*alt*-GA) owing to the cooperative H-bonding that originated from the contribution of the oxygen heteroatom in the DGA monomer. This study reveals how the combination of two monomers can significantly affect the properties of functional polyesters.

■ ASSOCIATED CONTENT

Supporting Information

The Supporting Information is available free of charge at https://pubs.acs.org/doi/10.1021/acsmacrolett.3c00104.

Additional analysis including ^{1}H and DOSY NMR, GPC, FT-IR, MALDI-ToF, and MD simulations (PDF)

■ AUTHOR INFORMATION

Corresponding Author

Byeong-Su Kim − *Department of Chemistry, Yonsei University, Seoul 03722, Republic of Korea;* orcid.org/0000-0002-6419-3054; Email: bskim19@yonsei.ac.kr

Authors

Sumin Lee − *Department of Chemistry, Yonsei University, Seoul 03722, Republic of Korea;* orcid.org/0000-0003-1928-7200

Woo Hyuk Jung − *Department of Chemical and Biological Engineering, Korea University, Seoul 02841, Republic of Korea;* orcid.org/0000-0001-5169-4223

Minseong Kim − *Department of Chemistry, Yonsei University, Seoul 03722, Republic of Korea;* orcid.org/0000-0002-2612-922X

Dong June Ahn − *Department of Chemical and Biological Engineering and KU-KIST Graduate School of Converging Science and Technology, Korea University, Seoul 02841, Republic of Korea;* orcid.org/0000-0001-5205-9168

Complete contact information is available at: https://pubs.acs.org/10.1021/acsmacrolett.3c00104

Author Contributions

CRediT: **Sumin Lee** conceptualization (lead), data curation (lead), formal analysis (lead), investigation (lead), visualization (lead), writing-original draft (lead), writing-review & editing (supporting); **Woo Hyuk Jung** formal analysis (supporting), validation (supporting), visualization (supporting), writing-original draft (supporting); **Minseong Kim** formal analysis (supporting), investigation (supporting), visualization (supporting); **Dong June Ahn** formal analysis (supporting), investigation (supporting), visualization (supporting), writing-original draft (supporting); **Byeong-Su Kim** conceptualization (lead), formal analysis (lead), funding acquisition (lead), investigation (supporting), project administration (lead), supervision (lead), visualization (supporting), writing-original draft (lead), writing-review & editing (lead).

Notes

The authors declare no competing financial interest.

■ ACKNOWLEDGMENTS

This work was supported by the National Research Foundation of Korea (NRF-2021R1A2C3004978 and NRF-2021M3H4A1A04092882).

■ REFERENCES

(1) MacLeod, M.; Arp, H. P. H.; Tekman, M. B.; Jahnke, A. The Global Threat from Plastic Pollution. *Science* **2021**, *373*, 61−65.

(2) Albertsson, A.-C.; Varma, I. K. Aliphatic Polyesters: Synthesis, Properties and Applications. In *Degradable Aliphatic Polyesters*; Springer: Berlin, 2002.

(3) Liu, X.; Desilles, N.; Lebrun, L. Polyesters from Renewable 1,4:3,6-Dianhydrohexitols for Food Packaging: Synthesis, Thermal, Mechanical and Barrier Properties. *Eur. Polym. J.* **2020**, *134*, 109846.

(4) Jadidi, A.; Salahinejad, E. Mechanical Strength and Biocompatibility of Bredigite (Ca7MgSi4O16) Tissue-Engineering Scaffolds Modified by Aliphatic Polyester Coatings. *Ceram. Int.* **2020**, *46*, 16439−16446.

(5) Seyednejad, H.; Ghassemi, A. H.; van Nostrum, C. F.; Vermonden, T.; Hennink, W. E. Functional Aliphatic Polyesters for Biomedical and Pharmaceutical Applications. *J. Controlled Release* **2011**, *152*, 168−176.

(6) Han, B.; Zhang, L.; Liu, B.; Dong, X.; Kim, I.; Duan, Z.; Theato, P. Controllable Synthesis of Stereoregular Polyesters by Organocatalytic Alternating Copolymerizations of Cyclohexene Oxide and Norbornene Anhydrides. *Macromolecules* **2015**, *48*, 3431−3437.

(7) Longo, J. M.; Sanford, M. J.; Coates, G. W. Ring-Opening Copolymerization of Epoxides and Cyclic Anhydrides with Discrete Metal Complexes: Structure−Property Relationships. *Chem. Rev.* **2016**, *116*, 15167−15197.

(8) Ryzhakov, D.; Printz, G.; Jacques, B.; Messaoudi, S.; Dumas, F.; Dagorne, S.; Le Bideau, F. Organo-Catalyzed/Initiated Ring Opening Co-Polymerization of Cyclic Anhydrides and Epoxides: An Emerging Story. *Polym. Chem.* **2021**, *12*, 2932−2946.

(9) Sanford, M. J.; Peña Carrodeguas, L.; Van Zee, N. J.; Kleij, A. W.; Coates, G. W. Alternating Copolymerization of Propylene Oxide and Cyclohexene Oxide with Tricyclic Anhydrides: Access to Partially Renewable Aliphatic Polyesters with High Glass Transition Temperatures. *Macromolecules* **2016**, *49*, 6394−6400.

(10) McGuire, T. M.; Clark, E. F.; Buchard, A. Polymers from Sugars and Cyclic Anhydrides: Ring-Opening Copolymerization of a D-Xylose Anhydrosugar Oxetane. *Macromolecules* **2021**, *54*, 5094−5105.

(11) Brandolese, A.; Della Monica, F.; Pericàs, M. À.; Kleij, A. W. Catalytic Ring-Opening Copolymerization of Fatty Acid Epoxides: Access to Functional Biopolyesters. *Macromolecules* **2022**, *55*, 2566−2573.

(12) Lee, J.; Han, S.; Kim, M.; Kim, B.-S. Anionic Polymerization of Azidoalkyl Glycidyl Ethers and Post-Polymerization Modification. *Macromolecules* **2020**, *53*, 355−366.

(13) Kim, M.; Mun, W.; Jung, W. H.; Lee, J.; Cho, G.; Kwon, J.; Ahn, D. J.; Mitchell, R. J.; Kim, B.-S. Antimicrobial PEGtides: A Modular Poly(Ethylene Glycol)-Based Peptidomimetic Approach to Combat Bacteria. *ACS Nano* **2021**, *15*, 9143−9153.

(14) Baek, J.; Kim, S.; Son, I.; Choi, S.-H.; Kim, B.-S. Hydrolysis-Driven Viscoelastic Transition in Triblock Copolyether Hydrogels with Acetal Pendants. *ACS Macro Lett.* **2021**, *10*, 1080−1087.

(15) Kim, M.; Park, J.; Lee, K. M.; Shin, E.; Park, S.; Lee, J.; Lim, C.; Kwak, S. K.; Lee, D. W.; Kim, B.-S. Peptidomimetic Wet-Adhesive PEGtides with Synergistic and Multimodal Hydrogen Bonding. *J. Am. Chem. Soc.* **2022**, *144*, 6261−6269.
(16) Park, J.; Yu, Y.; Lee, J. W.; Kim, B.-S. Anionic Ring-Opening Polymerization of a Functional Epoxide Monomer with an Oxazoline Protecting Group for the Synthesis of Polyethers with Carboxylic Acid Pendants. *Macromolecules* **2022**, *55*, 5448−5458.
(17) Kwon, G.; Kim, M.; Jung, W. H.; Park, S.; Tam, T.-T. H.; Oh, S.-H.; Choi, S.-H.; Ahn, D. J.; Lee, S.-H.; Kim, B.-S. Designing Cooperative Hydrogen Bonding in Polyethers with Carboxylic Acid Pendants. *Macromolecules* **2021**, *54*, 8478−8487.
(18) Xue, Y.-N.; Huang, Z.-Z.; Zhang, J.-T.; Liu, M.; Zhang, M.; Huang, S.-W.; Zhuo, R.-X. Synthesis and Self-Assembly of Amphiphilic Poly(Acrylic Acid-*b*-DL-Lactide) to Form Micelles for pH-Responsive Drug Delivery. *Polymer* **2009**, *50*, 3706−3713.
(19) Teng, L.; Chen, Y.; Jin, M.; Jia, Y.; Wang, Y.; Ren, L. Weak Hydrogen Bonds Lead to Self-Healable and Bioadhesive Hybrid Polymeric Hydrogels with Mineralization-Active Functions. *Biomacromolecules* **2018**, *19*, 1939−1949.
(20) Zhang, R.; Ruan, H.; Fu, Q.; Zhu, X.; Yao, Y. A High Strain, Adhesive, Self-Healable Poly(Acrylic Acid) Hydrogel with Temperature Sensitivity as an Epidermal Sensor. *Mater. Adv.* **2020**, *1*, 329−333.
(21) Wu, J.; Yuk, H.; Sarrafian, T. L.; Guo, C. F.; Griffiths, L. G.; Nabzdyk, C. S.; Zhao, X. An Off-the-Shelf Bioadhesive Patch for Sutureless Repair of Gastrointestinal Defects. *Sci. Transl. Med.* **2022**, *14*, eabh2857.
(22) Tian, M.; Chen, X.; Sun, S. T.; Yang, D.; Wu, P. Y. A Bioinspired High-Modulus Mineral Hydrogel Binder for Improving the Cycling Stability of Microsized Silicon Particle-Based Lithium-Ion Battery. *Nano Research* **2019**, *12*, 1121−1127.
(23) Zhang, B.; Li, H.; Luo, H.; Zhao, J. Ring-Opening Alternating Copolymerization of Epichlorohydrin and Cyclic Anhydrides Using Single- and Two-Component Metal-Free Catalysts. *Eur. Polym. J.* **2020**, *134*, 109820.
(24) Li, H.; Zhao, J.; Zhang, G. Self-Buffering Organocatalysis Tailoring Alternating Polyester. *ACS Macro Lett.* **2017**, *6*, 1094−1098.
(25) Li, H.; Luo, H.; Zhao, J.; Zhang, G. Well-Defined and Structurally Diverse Aromatic Alternating Polyesters Synthesized by Simple Phosphazene Catalysis. *Macromolecules* **2018**, *51*, 2247−2257.
(26) Meimoun, J.; Favrelle-Huret, A.; Winter, J. D.; Zinck, P. Poly(L-lactide) Epimerization and Chain Scission in the Presence of Organic Bases. *Macromol.* **2022**, *2*, 236−246.
(27) Xia, X.; Gao, T.; Li, F.; Suzuki, R.; Isono, T.; Satoh, T. Sequential Polymerization from Complex Monomer Mixtures: Access to Multiblock Copolymers with Adjustable Sequence, Topology, and Gradient Strength. *Macromolecules* **2023**, *56*, 92−103.
(28) Ghosh, S.; Glöckler, E.; Wölper, C.; Linders, J.; Janoszka, N.; Gröschel, A. H.; Schulz, S. Comparison of the Catalytic Activity of Mono- and Multinuclear Ga Complexes in the Rocop of Epoxides and Cyclic Anhydrides. *Eur. J. Inorg. Chem.* **2022**, *2022*, e202101017.
(29) Li, H.; He, G.; Chen, Y.; Zhao, J.; Zhang, G. One-Step Approach to Polyester−Polyether Block Copolymers Using Highly Tunable Bicomponent Catalyst. *ACS Macro Lett.* **2019**, *8*, 973−978.
(30) Luo, H.; Zhou, Y.; Li, Q.; Zhang, B.; Cao, X.; Zhao, J.; Zhang, G. Oxygenated Boron Species Generated in Situ by Protonolysis Enables Precision Synthesis of Alternating Polyesters. *Macromolecules* **2023**, *56*, 1907−1920.
(31) Filippov, A. D.; van Hees, I. A.; Fokkink, R.; Voets, I. K.; Kamperman, M. Rapid and Quantitative De-Tert-Butylation for Poly(Acrylic Acid) Block Copolymers and Influence on Relaxation of Thermoassociated Transient Networks. *Macromolecules* **2018**, *51*, 8316−8323.
(32) Tian, S.; Cao, X.; Luo, K.; Lin, Y.; Wang, W.; Xu, J.; Guo, B. Effects of Nonhydroxyl Oxygen Heteroatoms in Diethylene Glycols on the Properties of 2,5-Furandicarboxylic Acid-Based Polyesters. *Biomacromolecules* **2021**, *22*, 4823−4832.

https://doi.org/10.1021/acsmacrolett.3c00104
ACS Macro Lett. 2023, 12, 590−597